DALTON
FULL PAPER

Do the discrete dianions $C_2B_9H_{11}^{2-}$ exist? Characterisation of alkali metal salts of the 11-vertex *nido* dicarboranes, $C_2B_9H_{11}^{2-}$, in solution†

Mark A. Fox,* Andrew K. Hughes,* Andrew L. Johnson and Michael A. J. Paterson

Chemistry Department, Durham University Science Laboratories, South Road, Durham, UK DH1 3LE

Received 26th October 2001, Accepted 18th February 2002
First published as an Advance Article on the web 28th March 2002

Detailed experimental solution-state NMR data are reported for the nine moisture-sensitive salts of $M_2C_2B_9H_{11}$ (M = Li, Na, K) **1**–**9** generated by deprotonation of 7,8-$C_2B_9H_{13}$, 7,9-$C_2B_9H_{12}^-$ and 2,9-$C_2B_9H_{13}$ by butyllithium, sodium hydride and potassium hydride. Indicative of cation–anion interactions, the ^{11}B, ^{13}C and ^1H chemical shifts depend on the identity of the cation and, to a lesser degree, the solvent. Computed NMR shifts generated from MP2-optimised geometries of $C_2B_9H_{11}^{2-}$, $LiC_2B_9H_{11}^-$ and $NaC_2B_9H_{11}^-$ suggest that intimate ion-pair cluster anions $MC_2B_9H_{11}^-$ are present in solutions of $M_2C_2B_9H_{11}$. As a test of the method of comparing experimental structures and chemical shifts with those from optimised geometries, the optimised geometries of the small carborane alkali metal salts $M_2C_2B_4H_4(SiR_3)_2$ (M = Li or Na, R = H or Me) were computed and shown to agree well with experimental structures.

Introduction

Alkali metal salts of the carborane dianions 7,8-, 7,9- and 2,9-$C_2B_9H_{11}^{2-}$ **A–C**, Fig. 1, generated *in situ* by deprotonation of

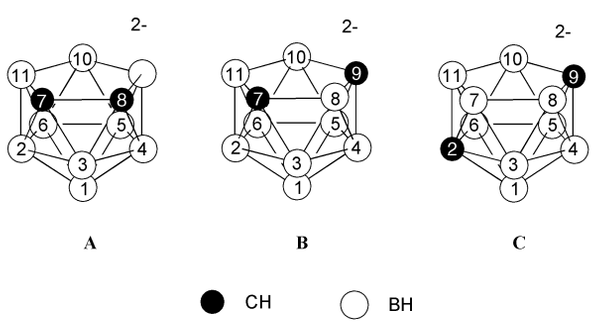

Fig. 1 Numbering of cage atoms of the three *nido*-carborane dianions 7,8-$C_2B_9H_{11}^{2-}$ **A**, 7,9-$C_2B_9H_{11}^{2-}$ **B** and 2,9-$C_2B_9H_{11}^{2-}$ **C**.

their respective monoanions $C_2B_9H_{12}^-$ are precursors to an enormous number of metallacarboranes.[1–5] These salts $M_2C_2B_9H_{11}$ (M = Li, Na, K, Cs) and related tetraalkylammonium salts are frequently considered to contain discrete dianions with formulae $(M^+)_2(C_2B_9H_{11}^{2-})$.[6] However, characterisation data on these air-sensitive salts are sparse. In fact the only reported characterising data for the alkali metal salts $M_2C_2B_9H_{11}$ are the ^{11}B and ^1H NMR data in THF-d_8 for Li_2(7,8-$C_2B_9H_{11}$) **1**, the ^{11}B NMR spectrum showing resonances in a 3 : 3 : 2 : 1 ratio,[7] and the ^{11}B NMR spectrum of Na_2(7,8-$C_2B_9H_{11}$) **2** in THF which shows four resonances in a 6 : 1 : 1 : 1 ratio, with the chemical shifts not reported.[8] The differing ^{11}B NMR patterns reported for salts containing different cations with the same dianion 7,8-$C_2B_9H_{11}^{2-}$ suggest some interaction between the dianion and cation. Prior to this study the alkali metal salts K_2(7,8-$C_2B_9H_{11}$) **3**, M_2(7,9-$C_2B_9H_{11}$) **4**–**6** and M_2(2,9-$C_2B_9H_{11}$) **7**–**9** (M = Li, Na and K respectively) had not been characterised.

By contrast, alkali metal salts of the related small carborane dianions 2,3-$(Me_3Si)_2$-2,3-$C_2B_4H_4^{2-}$ **D** and 2,4-$(Me_3Si)_2$-2,4-$C_2B_4H_4^{2-}$ **E**, Fig. 2, are well characterised.[9,10] These may be

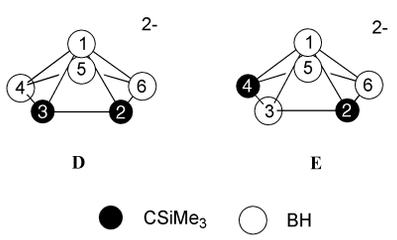

Fig. 2 Numbering of cage atoms of the two *nido*-carborane dianions 2,3-$(Me_3Si)_2$-2,3-$C_2B_4H_4^{2-}$ **D** and 2,4-$(Me_3Si)_2$-2,4-$C_2B_4H_4^{2-}$ **E**.

viewed as 7,8-$C_2B_9H_{11}^{2-}$ **A** and 7,9-$C_2B_9H_{11}^{2-}$ **B** cages respectively with the B_5H_5 (B2–B6) belt removed and hydrogen atoms at carbons replaced by Me_3Si groups. Molecular structures of the salts [Li(TMEDA)]$_2$[2,3-$(Me_3Si)_2$-2,3-$C_2B_4H_4$] **10**,[9] [Li(TMEDA)]$_2$[2,4-$(Me_3Si)_2$-2,4-$C_2B_4H_4$] **11**,[10] [Li(THF)]$_2$[2,4-$(Me_3Si)_2$-2,4-$C_2B_4H_4$] **12**[10] and [Na(THF)$_2$]$_2$[2,4-$(Me_3Si)_2$-2,4-$C_2B_4H_4$] **13**,[11] show one of the metal atoms to occupy an apical position above the C_2B_3 face and the second metal atom to be *exo*-bonded to the cage (Fig. 3). For the di-lithium salts of 2,3-$C_2B_4H_6^{2-}$ and 2,4-$C_2B_4H_6^{2-}$, a recent geometry optimisation and computed NMR study suggests that intimate ion-pair cluster anions are present in solution with the lithium atom at the apical position.[12,13] Recently, alkali metal salts of twelve-vertex carborane dianions containing six-membered open faces were structurally characterised.[14]

Following our recent structural studies[15] of the protonated Proton Sponge [1,8-bis(dimethylamino)naphthalene] salts of 7,8- 7,9- and 2,9-*nido*-$C_2B_9H_{12}^-$ we have directed our attention to the structures of the related dianions. Given the lack of structural data available on the alkali metal salts of $C_2B_9H_{11}^{2-}$, and the absence of suitable crystals for diffraction studies, we have chosen to record the solution-state NMR data for these anions as a range of salts in different solvents. Here we report

† Electronic supplementary information (ESI) available: selected bond lengths of optimised model geometries of **H** and **I**. COSY spectrum of **4**. Compiled NMR data and Cartesian coordinates for MP2/6–31G* geometries of 7,8-Me_2-7,8-$C_2B_9H_{10}^-$. Rotatable 3-D molecular structure diagrams of optimised geometries **A** to **FF** in CHIME format. See http://www.rsc.org/suppdata/dt/b1/b109804g/

DOI: 10.1039/b109804g

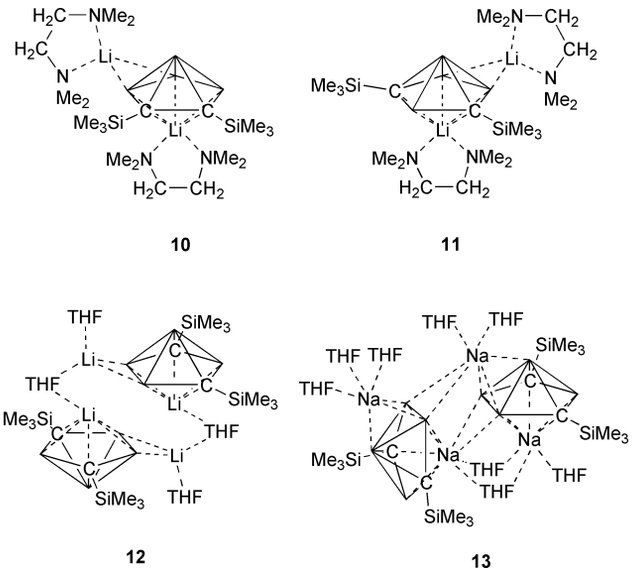

Fig. 3 Schematic solid-state geometries of *exo*-(TMEDA)Li-*ap*-(TMEDA)Li-2,3-$(Me_3Si)_2$-2,3-$C_2B_4H_4$ **10**, 5,6-*exo*-(TMEDA)Li-*ap*-(TMEDA)Li-2,4-$(Me_3Si)_2$-2,4-$C_2B_4H_4$ **11**, $[Li(THF)]_2$[2,4-$(Me_3Si)_2$-2,4-$C_2B_4H_4$] **12** dimer and $[Na(THF)_2]_2$[2,4-$(Me_3Si)_2$-2,4-$C_2B_4H_4$] **13** dimer.

experimental NMR spectroscopic data for the salts $M_2C_2B_9H_{11}$, M = Li, Na and K **1**–**9**, in a range of solvents. We also discuss the most likely structures of $M_2C_2B_9H_{11}$ and the smaller cage analogues $M_2C_2B_4H_4(SiMe_3)_2$ by comparison between the NMR shifts observed experimentally and those calculated from MP2-optimised model geometries.

Experimental

NMR spectra including 2D ^{11}B–$^{11}B\{^1H\}$ COSY and $^1H\{^{11}B$ selective$\}$ were recorded on Varian Unity 300 (299.9 MHz ^1H, 96.2 MHz ^{11}B and 75.4 MHz ^{13}C) or Varian Inova 500 (194.2 MHz ^7Li and 160.3 MHz ^{11}B) instruments. ^1H NMR spectra were referenced to residual protio impurity in the solvent (CD_2HCN, 1.95 ppm; C_5D_4HN, 8.62, 7.68, 7.29; C_6D_5H, 7.15). ^{13}C NMR spectra were referenced to the solvent resonance (CD_3CN, 118.2, 1.3 ppm; C_5D_5N, 150.0, 123.8, 136; C_6D_6, 128.0). ^{11}B NMR spectra were referenced externally to $Et_2O{\cdot}BF_3$ in Et_2O, δ = 0.0 ppm whereas ^7Li NMR spectra were referenced externally to 1M LiCl in D_2O, δ = 0.0 ppm.

Ortho, *meta* and *para*-carborane (Katchem) were purified by sublimation under vacuum. The carboranes 7,8-$C_2B_9H_{13}$,[16] $(HNMe_3)$(*nido*-7,9-$C_2B_9H_{12}$),[17] $(HNMe_3)$(7,8-Me_2-7,8-$C_2B_9H_{10}$)[17] and *nido*-2,9-$C_2B_9H_{13}$[18] were prepared as described in the literature. A mixed solvent consisting of 10% by volume C_6D_6 in THF was prepared from dried solvents, THF was dried by distillation from molten potassium, C_6D_6 was dried by distillation from CaH_2.

Synthesis of the lithium salt $Li_2(7,8\text{-}C_2B_9H_{11})$ 1

A toluene (20 ml) solution of 7,8-$C_2B_9H_{13}$ (0.2 g, 1.5 mmol) was treated dropwise at 0 °C with a solution of BuLi (1.6 M in hexane, 1.9 ml, 3 mmol), forming a white precipitate. After stirring for 12 h at ambient temperature the solution was refluxed for 4 h. The solvent was removed under reduced pressure and the residue remained under vacuum for an hour. The solid was washed twice with anhydrous hexane (10 ml). The air-sensitive white residue was then left to dry under vacuum (0.05 mmHg) for 12 h and identified by NMR spectroscopy (Table 1) as the di-lithium salt $Li_2(7,8\text{-}C_2B_9H_{11})$ (92%, 0.21 g).

Synthesis of the lithium salt $Li_2(7,9\text{-}C_2B_9H_{11})$ 4

This procedure was adapted from the reported synthesis of the di-lithium salt $Li_2(7,8\text{-}C_2B_9H_{11})$ from $(Me_3NH)(7,8\text{-}C_2B_9H_{12})$.[19] The Me_3NH^+ salt of 7,9-$C_2B_9H_{12}^-$ (0.3 g, 1.5 mmol) was stirred under N_2 in 20 ml of an 1 : 1 ratio mixture of anhydrous Et_2O : toluene. A solution of BuLi (1.6 M in hexane, 1.9 ml, 3 mmol) was added dropwise at 0 °C, and the mixture was then stirred for a further 24 h at ambient temperature, then finally refluxed for 4 h. The reaction mixture was then cooled, the solvent was removed under reduced pressure and the residue dried under vacuum (0.05 mmHg) for 1 h. Anhydrous hexane (10 ml) was added to the white residue, the suspension was stirred for 1 h and the hexane solution was then removed using a cannula. The washing procedure with hexane was repeated twice. The resulting white air-sensitive solid was dried under vacuum for 12 h and the di-lithium salt $Li_2(7,9\text{-}C_2B_9H_{11})$ (89%, 0.19 g) was identified by NMR spectroscopy (see Table 2).

Synthesis of the lithium salt $Li_2(2,9\text{-}C_2B_9H_{11})$ 7

Using the same procedure as for the synthesis of $Li_2(7,8\text{-}C_2B_9H_{11})$, the neutral carborane 2,9-$C_2B_9H_{13}$ (0.2 g, 1.5 mmol) gave the air-sensitive white solid identified by NMR spectroscopy (see Table 3) as the di-lithium salt $Li_2(2,9\text{-}C_2B_9H_{11})$ (97%, 0.22 g).

NMR tube reactions

Short Pyrex extensions were attached to Pyrex NMR tubes, enabling the tubes to be sealed by freezing the solution in the tube by immersing in liquid nitrogen, evacuating the remainder of the tube, then sealing with a blowtorch.

General preparation for sodium and potassium salts

A solution of the *nido*-carborane, 7,8-$C_2B_9H_{13}$, $(HNMe_3)$-(7,8-Me_2-7,8-$C_2B_9H_{10}$), $(HNMe_3)$(7,9-$C_2B_9H_{12}$) or 2,9-$C_2B_9H_{13}$ (0.05 mmol) in 0.5 ml of pyridine-d_5 or THF–10% C_6D_6 was added slowly to an excess of washed (light petroleum ether, bp 40–60 °C) and dried metal hydride NaH or KH in a NMR tube. When the initial evolution of gas ceased the NMR tube was sealed under vacuum. The ^{11}B NMR spectrum was recorded, and if mono anion was present in the spectrum the tube was heated at 50 °C for three hours.

Computational section

All *ab initio* computations were carried out with the Gaussian 94 and 98 packages.[20,21] The geometries discussed here were optimised at the HF/6-31G* level with no symmetry constraints. Frequency calculations were computed on these optimised geometries at the HF/6-31G* level for imaginary frequencies – none were found. Optimisations of these geometries were then carried out at the computationally intensive MP2/6-31G* level and NMR shifts calculated at the GIAO-B3LYP/6-311G* level. Theoretical ^{11}B chemical shifts at the GIAO-B3LYP/6-311G*//MP2/6-31G* level listed in the tables have been referenced to B_2H_6 (16.6 ppm[22]) and converted to the usual $BF_3{\cdot}OEt_2$ scale: $\delta(^{11}B) = 102.83 - \sigma(^{11}B)$. The ^{13}C and ^1H chemical shifts were referenced to TMS: $\delta(^{13}C) = 184.81 - \sigma(^{13}C)$; $\delta(^1H) = 32.28 - \sigma(^1H)$. Relative energies were computed at the MP2/6-31G* level with ZPE (calculated at HF/6-31G*) corrections scaled by 0.89. The root mean squared fitting method used for comparison of experimental and theoretical geometries was carried out using the *ofit* command in the *xp* program as part of the SHELXL package.[23]

See ESI † for xyz files containing Cartesian coordinates of the optimised geometries of **A** to **FF**.

Results and discussion

Experimental studies

Acetonitrile-d_3 solutions of the di-lithium salts $Li_2C_2B_9H_{11}$ **1**, **4** and **7** were prepared by dissolving freshly prepared samples,

Table 1 Observed (values in bold) and calculated ^{11}B, ^{13}C, ^{7}Li and ^{1}H NMR shifts for derivatives containing the 7,8-$C_2B_9H_{11}$ moiety

Formula and compound number		^{11}B[a]						^{13}C	^{7}Li	
$Li_2(C_2B_9H_{11})$ in CD_3CN	**1**	**−17.2 (B10)**	**−17.2 (*B5,6*)**	**−19.2 (B9,11)**	**−21.5 (B3)**	**−24.5 (*B2,4*)**	**−41.8 (B1)**	**33.1**	**2.88 *ap* Li**	**1.59 *exo* Li**
$Li_2(C_2B_9H_{11})$ in THF–C_6D_6	**1**	**−18.9 (1B)**	**−18.9 (2B)**	**−20.1 (2B)**	**−20.1 (1B)**	**−24.6 (2B)**	**−42.4 (B1)**	**32.5**	**−2.40 *ap* Li**	**−3.33 *exo* Li**
$Na_2(C_2B_9H_{11})$ in C_5D_5N	**2**	**−19.2 (2B)**	**−19.2 (2B)**	**−19.2 (*B3*)**	**−21.0 (1B)**	**−24.8 (*B2,4*)**	**−45.0 (B1)**	**31.5**		
$Na_2(C_2B_9H_{11})$ in THF–C_6D_6	**2**	**−21.4 (2B)**	**−21.4 (2B)**	**−21.4 (1B)**	**−24.3 (1B)**	**−26.2 (2B)**	**−47.0 (B1)**	**31.0**		
$K_2(C_2B_9H_{11})$ in C_5D_5N	**3**	**−18.5 (2B)**	**−18.5 (2B)**	**−18.5 (1B)**	**−24.2 (1B)**	**−24.2 (*B2,4*)**	**−45.0 (B1)**	**31.5**		
$K_2(C_2B_9H_{11})$ in THF–C_6D_6	**3**	**−20.3 (2B)**	**−20.3 (2B)**	**−20.3 (1B)**	**−25.0 (1B)**	**−25.0 (2B)**	**−46.3 (B1)**			
7,8-$C_2B_9H_{11}^{2-}$	**A**	−20.9 (B10)	−21.3 (B5,6)	−23.0 (B9,11)	−26.2 (B3)	−29.7 (B2,4)	−51.4 (B1)	30.1		
ap-Li-7,8-$C_2B_9H_{11}^{-}$	**X**	−13.3 (B10)	−14.6 (B5,6)	−19.4 (B9,11)	−22.4 (B3)	−24.4 (B2,4)	−38.1 (B1)	39.7		
ap-Na-7,8-$C_2B_9H_{11}^{-}$	**AA**	−18.4 (B5,6)	−22.4 (B10)	−23.0 (B3)	−24.2 (B9,11)	−26.8 (B2,4)	−47.3 (B1)	36.5		
5,6,10-*exo*-Li-*ap*-Li-7,8-$C_2B_9H_{11}$	**DD**	−17.6 (B3)	−17.6 (B9,11)	−19.1 (B5,6)	−21.6 (B10)	−25.4 (B2,4)	−37.9 (B1)	44.4		

		^{1}H[b]						
$Li_2(C_2B_9H_{11})$ in CD_3CN	**1**	**1.80 (B3H)**	**0.93 (*B2,4H*)**	**0.86 (B9,11H)**	**0.74 (*B5,6H*)**	**0.41 (B10H)**	**0.03 (B1H)**	**1.08 (CH)**
$Na_2(C_2B_9H_{11})$ in C_5D_5N	**2**	**2.71 (*B3H*)**	**2.29 (*B2,4H*)**	**2.15 (2H)(−19.2)**[c]	**1.97 (2H)(−19.2)**[c]	**1.42 (1H)(−21.0)**[c]	**1.38 (B1H)**	**1.63 (CH)**
$K_2(C_2B_9H_{11})$ in C_5D_5N	**3**	**2.59 (B3H)**	**2.09 (B2,4H)**	**1.82 (2H)(−18.5)**[c]	**1.71 (2H)(−18.5)**[c]	**1.21 (1H)(−24.2)**[c]	**1.16 (B1H)**	**1.55 (CH)**
7,8-$C_2B_9H_{11}^{2-}$	**A**	1.68 (B3H)	1.07 (B9,11H)	1.06 (B2,4H)	1.01 (B5,6H)	0.73 (B10H)	0.05 (B1H)	0.16 (CH)
ap-Li-7,8-$C_2B_9H_{11}^{-}$	**X**	2.16 (B3H)	1.67 (B2,4H)	1.67 (B5,6H)	1.67 (B10H)	1.53 (B9,11H)	1.17 (B1H)	1.14 (CH)
ap-Na-7,8-$C_2B_9H_{11}^{-}$	**AA**	2.04 (B3H)	1.54 (B2,4H)	1.45 (B5,6H)	1.39 (B9,11H)	1.00 (B10H)	0.80 (B1H)	0.69 (CH)
5,6,10-*exo*-Li-*ap*-Li-7,8-$C_2B_9H_{11}$	**DD**	2.65 (B3H)	2.15 (B9,11H)	2.07 (B2,4H)	1.68 (B1H)	1.13 (B5,6H)	0.39 (B10H)	1.64 (CH)

[a] Experimental data has been assigned by ^{11}B–^{11}B COSY. Values in italic cannot be uniquely assigned by COSY, the given assignments are by comparison with the calculated data. [b] Assignments given in italics are uncertain because the attached boron atom has not been uniquely assigned. [c] Value in parentheses indicates the ^{11}B chemical shift with which this proton is correlated.

Table 2 Observed (values in bold) and calculated ^{11}B, ^{13}C, ^{7}Li and ^{1}H NMR shifts NMR shifts for derivatives containing the 7,9-$C_2B_9H_{11}$ moiety

Formula and compound number		^{11}B [a]						^{13}C	^{7}Li	
$Li_2(C_2B_9H_{11})$ in CD_3CN	**4**	**−17.5 (*B2,5*)**	**−19.8 (B10,11)**	**−21.5 (B8)**	**−22.9 (*B3,4*)**	**−22.9 (B6)**	**−42.5 (B1)**	**32.6**	**2.66 *ap* Li**	**2.11 *exo* Li**
$Li_2(C_2B_9H_{11})$ in THF–C_6D_6	**4**	**−18.0 (B2,5)**	**−20.7 (B8)**	**−21.2 (B10,11)**	**−22.9 (B3,4)**	**−24.2 (B6)**	**−43.1 (B1)**	**30.4**	**−2.81**	**−2.81**
$Na_2(C_2B_9H_{11})$ in C_5D_5N	**5**	**−18.5 (2B)**	**−18.5 (1B)**	**−21.4 (2B)**	**−22.4 (2B)**	**−24.0 (1B)**	**−46.8 (B1)**	**33.0**		
$Na_2(C_2B_9H_{11})$ in THF–C_6D_6	**5**	**−19.8 (2B)**	**−19.8 (1B)**	**−23.4 (2B)**	**−23.9 (2B)**	**−26.4 (1B)**	**−48.8 (B1)**	**32.2**		
$K_2(C_2B_9H_{11})$ in C_5D_5N	**6**	**−17.9 (2B)**	**−17.9 (1B)**	**−19.6 (2B)**	**−22.5 (2B)**	**−22.5 (1B)**	**−45.9 (B1)**			
$K_2(C_2B_9H_{11})$ in THF–C_6D_6	**6**	**−19.3 (2B)**	**−19.3 (1B)**	**−24.9 (2B)**	**−24.9 (2B)**	**−24.9 (1B)**	**−47.9 (B1)**			
7,9-$C_2B_9H_{11}^{2-}$	**B**	−21.7 (B2,5)	−23.8 (B8)	−24.2 (B10,11)	−25.6 (B6)	−26.9 (B3,4)	−53.8 (B1)	26.1		
ap-Li-7,9-$C_2B_9H_{11}^{-}$	**Y**	−16.3 (B2,5)	−19.2 (B10,11)	−20.2 (B6)	−22.4 (B3,4)	−22.7 (B8)	−39.5 (B1)	42.5		
ap-Na-7,9-$C_2B_9H_{11}^{-}$	**BB**	−18.4 (B2,5)	−20.3 (B8)	−24.0 (B6)	−24.0 (B10,11)	−24.2 (B3,4)	−49.3 (B1)	31.4		
6,10,11-*exo*-Li-*ap*-Li-7,9-$C_2B_9H_{11}$	**EE**	−13.3 (B2,5)	−16.5 (B8)	−17.5 (B3,4)	−25.8 (B6)	−25.4 (B10,11)	−37.9 (B1)	41.3		

		^{1}H [b]						
$Li_2(C_2B_9H_{11})$ in CD_3CN	**4**	**1.18 (*B2,5H*)**	**0.96 (*B3,4H*)**	**0.72 (B10,11H)**	**0.47 (B6H)**	**0.19 (B8H)**	**−0.14 (B1H)**	**0.19 (CH)**
$Na_2(C_2B_9H_{11})$ in C_5D_5N	**5**	**2.53 (1H) (−18.5)** [c]	**2.44 (2H) (−18.5)** [c]	**2.38 (2H) (−22.4)** [c]	**1.88 (2H) (−21.4)** [c]	**1.77 (1H) (−24.0)** [c]	**1.15 (B1H)**	**1.19 (CH)**
$K_2(C_2B_9H_{11})$ in C_5D_5N	**6**	**2.42 (1H) (−17.9)** [c]	**2.34 (2H) (−17.9)** [c]	**2.31 (2H) (−22.5)** [c]	**1.71 (2H) (−19.6)** [c]	**1.64 (1H) (−22.5)** [c]	**1.14 (B1H)**	**1.10 (CH)**
7,9-$C_2B_9H_{11}^{2-}$	**B**	1.47 (B2,5H)	1.28 (B8H)	1.24 (B3,4H)	0.94 (B10,11H)	0.91 (B6H)	−0.20 (B1H)	−0.48 (CH)
ap-Li-7,9-$C_2B_9H_{11}^{-}$	**Y**	2.02 (B2,5H)	1.81 (B3,4H)	1.70 (B8H)	1.57 (B10,11H)	1.49 (B6H)	1.02 (B1H)	0.72 (CH)
ap-Na-7,9-$C_2B_9H_{11}^{-}$	**BB**	1.92 (B2,5H)	1.68 (B3,4H)	1.35 (B8H)	1.30 (B10,11H)	1.24 (B6H)	0.57 (B1H)	0.35 (CH)
6,10,11-*exo*-Li-*ap*-Li-7,9-$C_2B_9H_{11}$	**EE**	2.65 (B2,5H)	2.36 (B3,4H)	2.35 (B8H)	1.62 (B1H)	1.09 (B10,11H)	0.88 (B6H)	1.23 (CH)

[a] Experimental data has been assigned by ^{11}B–^{11}B COSY. Values in italic cannot be uniquely assigned by COSY, the given assignments are by comparison with the calculated data. [b] Assignments given in italics are uncertain because the attached boron atom has not been uniquely assigned. [c] Value in parentheses indicates the ^{11}B chemical shift with which this proton is correlated.

Table 3 Observed (values in bold) and calculated NMR shifts for derivatives containing the 2,9-$C_2B_9H_{11}$ moiety

		^{11}B[a]					^{13}C		^{7}Li	
$Li_2(C_2B_9H_{11})$ in CD_3CN	**7**	**−21.5 (*B4,5*)**	**−22.2 (*B7,11*)**	**−23.6 (*B3,6*)**	**−24.3 (*B8,10*)**	**−43.9 (B1)**	**43.7 (C2)**	**37.1 (C9)**	**2.80 *ap* Li**	**2.52 *exo* Li**
$Li_2(C_2B_9H_{11})$ in THF–C_6D_6	**7**	**−21.5**	**−23.7**	**−23.7**	**−24.6**	**−44.7 (B1)**	**43.3**	**36.0**	**−2.67**	**−2.67**
$Na_2(C_2B_9H_{11})$ in C_5D_5N	**8**	**−21.7**	**−23.9**	**−24.9**	**−24.9 (*B7,11*)**	**−49.3 (B1)**	**38.6**	**32.8**		
$Na_2(C_2B_9H_{11})$ in THF–C_6D_6	**8**	**−23.9**	**−25.1**	**−26.2**	**−27.8**	**−50.8 (B1)**	**37.5**	**31.5**		
$K_2(C_2B_9H_{11})$ in C_5D_5N	**9**	**−20.8**	**−23.7**	**−23.7**	**−23.7 (*B7,11*)**	**−49.1 (B1)**				
$K_2(C_2B_9H_{11})$ in THF–C_6D_6	**9**	**−22.3**	**−24.3**	**−24.3**	**−24.3**	**−49.7 (B1)**				
2,9-$C_2B_9H_{11}^{2-}$	**C**	−26.6 (B8,10)	−28.3 (B4,5)	−29.1 (B3,6)	−31.5 (B7,11)	−57.8 (B1)	41.4 (C2)	27.6 (C9)		
ap-Li-2,9-$C_2B_9H_{11}^{-}$	**Z**	−21.3 (B8,10)	−22.3 (B7,11)	−23.3 (B4,5)	−24.8 (B3,6)	−42.8 (B1)	53.1 (C2)	47.0 (C9)		
ap-Na-2,9-$C_2B_9H_{11}^{-}$	**CC**	−24.0 (B8,10)	−25.3 (B4,5)	−28.2 (B3,6)	−30.4 (B7,11)	−51.9 (B1)	46.8 (C2)	36.6 (C9)		
3,7,8-*exo*-Li-*ap*-Li-2,9-$C_2B_9H_{11}$	**FF**	−19.5 (B4,5)	−21.1 (B8,10)	−24.7 (B3,6)	−25.0 (B7,11)	−41.9 (B1)	55.8 (C2)	45.9 (C9)		

		^{1}H[b]						
$Li_2(C_2B_9H_{11})$ in CD_3CN	**7**	**1.10 (*B3,6H*)**	**0.95 (*B8,10H*)**	**0.70 (*B4,5H*)**	**0.41 (B1H)**	**0.07 (*B7,11H*)**	**1.31 (*C2H*)**	**−0.01 (*C9H*)**
$Na_2(C_2B_9H_{11})$ in C_5D_5N	**8**	**2.50 (−23.9)**[c]	**2.37 (−24.9)**[c]	**2.08 (−21.7)**[c]	**1.50 (B1H)**	**0.80 (*B7,11H*)**	**1.35 (C2H)**	**0.25 (C9H)**
$K_2(C_2B_9H_{11})$ in C_5D_5N	**9**	**2.33 (−23.7)**[c]	**2.14 (−23.7)**[c]	**1.76 (−20.8)**[c]	**1.34 (B1H)**	**0.90 (*B7,11H*)**	**1.35 (C2H)**	**0.33 (C9H)**
2,9-$C_2B_9H_{11}^{2-}$	**C**	1.25 (B4,5H)	1.16 (B3,6H)	0.82 (B8,10H)	0.05 (B1H)	−0.08 (B7,11H)	0.89 (C2H)	−0.93 (C9H)
ap-Li-2,9-$C_2B_9H_{11}^{-}$	**Z**	1.89 (B4,5H)	1.70 (B3,6H)	1.40 (B8,10H)	1.23 (B1H)	0.99 (B7,11H)	0.98 (C2H)	0.46 (C9H)
ap-Na-2,9-$C_2B_9H_{11}^{-}$	**CC**	1.73 (B4,5H)	1.49 (B3,6H)	1.14 (B8,10H)	0.79 (B1H)	0.46 (B7,11H)	1.38 (C2H)	−0.04 (C9H)
3,7,8-*exo*-Li-*ap*-Li-2,9-$C_2B_9H_{11}$	**FF**	2.45 (B4,5H)	1.80 (B3,6H)	1.74 (B1H)	1.48 (B8,10H)	0.86 (B7,11H)	2.32 (C2H)	0.97 (C9H)

[a] Experimental data his been assigned by ^{11}B–^{11}B COSY. Values in italic cannot be uniquely assigned by COSY, the given assignments are by comparison with the calculated data. [b] Assignments given in italics are uncertain because the attached boron atom has not been uniquely assigned. [c] Value in parentheses indicates the ^{11}B chemical shift with which this proton is correlated.

Table 4 Observed (values in bold) and calculated ^{11}B NMR shifts for compounds containing the 2,3-$(R_3Si)_2$-2,3-$C_2B_4H_4^{2-}$ moiety

		B1	B5	B4[a]	B6 (av. B4/B6)[b]	Ref.
[(TMEDA)Li]$_2$[2,3-$(Me_3Si)_2$-2,3-$C_2B_4H_4$] in C_6D_6	**10**	**−48.4**	**3.2**	**18.2**		9
Li_2[2,3-$(Me_3Si)_2$-2,3-$C_2B_4H_4$] in C_6D_6	**14**	**−44.5**	**2.4**	**20.9**		9
2,3-$(Me_3Si)_2$-2,3-$C_2B_4H_4^{2-}$	**D**	−54.2	1.8	21.0		
exo-(en)Li-*ap*-(en)Li-2,3-$(H_3Si)_2$-2,3-$C_2B_4H_4$	**H**	−47.0	0.9	15.0	23.6 (19.3)	
4,5-*exo*-Li-*ap*-Li-2,3-$(H_3Si)_2$-2,3-$C_2B_4H_4$	**J**	−47.8	2.8	11.8	22.9 (17.4)	
ap-Li-2,3-$(Me_3Si)_2$-2,3-$C_2B_4H_4^-$	**L**	−47.8	8.6	21.2		
4,5-*exo*-Li-2,3-$(H_3Si)_2$-2,3-$C_2B_4H_4^-$	**P**	−55.0	1.1	10.4	21.7 (16.1)	
ap-Na-2,3-$(Me_3Si)_2$-2,3-$C_2B_4H_4^-$	**N**	−57.8	4.4	19.6		
exo-Na-*ap*-Na-2,3-$(H_3Si)_2$-2,3-$C_2B_4H_4$	**R**	−59.2	−2.8	11.2	22.5 (16.8)	
1,4,5-*exo*-Na-2,3-$(Me_3Si)_2$-2,3-$C_2B_4H_4^-$	**T**	−63.8	−4.7	6.8	20.2 (13.1)	

[a] B4 and B6 chemical shifts if equivalent by symmetry. [b] B6 chemical shift if not symmetry equivalent to B4, with the average of B4 and B6 in parentheses to allow for B4/B6 fluxionality.

Table 5 Observed (values in bold) and calculated boron NMR shifts for derivatives containing the 2,4-$(R_3Si)_2$-2,4-$C_2B_4H_4^{2-}$ moiety

		B1	B5,6	B3	Ref.
[(TMEDA)Li]$_2$[2,4-$(Me_3Si)_2$-2,4-$C_2B_4H_4$] in C_6D_6	**11**	**−48.8**	**6.5**	**18.0**	10
Li_2[2,4-$(Me_3Si)_2$-2,4-$C_2B_4H_4$] in THF	**12**	**−42.3**	**13.9**	**16.3**	10
Na_2[2,4-$(Me_3Si)_2$-2,4-$C_2B_4H_4$] in THF	**13**	**−45.9**	**8.1**	**30.0**	11
2,4-$(Me_3Si)_2$-2,4-$C_2B_4H_4^{2-}$	**E**	−58.4	6.4	10.4	
5,6-*exo*-(en)Li-*ap*-(en)Li-2,4-$(H_3Si)_2$-2,4-$C_2B_4H_4$	**I**	−49.4	7.0	18.3	
5,6-*exo*-Li-*ap*-Li-2,4-$(H_3Si)_2$-2,4-$C_2B_4H_4$	**K**	−52.1	6.7	21.0	
ap-Li-2,4-$(Me_3Si)_2$-2,4-$C_2B_4H_4^-$	**M**	−51.6	11.2	11.0	
5,6-*exo*-Li-2,4-$(H_3Si)_2$-2,4-$C_2B_4H_4^-$	**Q**	−56.0	1.7	27.1	
ap-Na-2,4-$(Me_3Si)_2$-2,4-$C_2B_4H_4^-$	**O**	−62.2	8.7	12.0	
1,5,6-*exo*-Na-*ap*-Na-2,4-$(H_3Si)_2$-2,4-$C_2B_4H_4$	**S**	−60.4	3.4	20.5	
1,5,6-*exo*-Na-2,4-$(Me_3Si)_2$-2,4-$C_2B_4H_4^-$	**U**	−62.1	−1.5	21.3	

Table 6 Observed (values in bold) and calculated boron NMR shifts for the 7,8-Me_2-7,8-$C_2B_9H_9$ moiety

		^{11}B					
$Na_2(Me_2C_2B_9H_9)$ in THF	**14**	**−12.2 (1B)**	**−18.9 (2B)**	**−22.6 (2B)**	**−22.6 (2B)**	**−27.3 (1B)**	**−46.4 (B1)**
7,8-Me_2-7,8-$C_2B_9H_9^{2-}$	**F**	−14.2 (B3)	−19.5 (B9,11)	−21.5 (B5,6)	−23.7 (B10)	−24.1 (B2,4)	−49.2 (B1)
ap-Na-7,8-Me_2-7,8-$C_2B_9H_9^-$	**G**	−13.1 (B3)	−17.9 (B9,11)	−20.3 (B5,6)	−21.8 (B10)	−24.0 (B2,4)	−40.6 (B1)

generated from BuLi and 7,8-$C_2B_9H_{13}$, $(HNMe_3)$(7,9-$C_2B_9H_{12}$) or 2,9-$C_2B_9H_{13}$, respectively. The ^{1}H, ^{11}B and ^{13}C NMR spectroscopic data for these salts are listed in Tables 1–3 together with assignments based on the results of ^{11}B–^{11}B{^{1}H} COSY and ^{1}H{^{11}B-selective} double resonance experiments where possible.

Solutions of the di-sodium and di-potassium salts cannot be produced in acetonitrile, since the solvent is prone to deprotonation and/or nucleophilic attack by either $M_2C_2B_9H_{11}$, or by excess metal hydride if this is employed for *in situ* deprotonation in the NMR tube. Solutions of the sodium and potassium salts were prepared in pyridine-d_5, by *in situ* reaction of an excess of NaH or KH with the same carborane precursors. Following the initial rapid evolution of one equivalent of hydrogen, the NMR tubes were sealed under vacuum and heated to 50 °C to complete the reaction. The presence of an excess of metal hydride was found to be necessary to ensure complete conversion into the desired salts.

Solution NMR data for the di-sodium (**2**, **5** and **8**) and di-potassium salts (**3**, **6** and **9**) recorded in pyridine-d_5 are also listed in Tables 1–3. There is a significant increase in line width for the sodium and especially the potassium salts relative to the sharper spectra obtained for the lithium salts. While peak information can be gleaned from the selective ^{1}H{^{11}B} spectra for these salts, 2D ^{11}B–^{11}B COSY spectra revealed no cross peaks. This absence is attributed to an increase in the size of the boron containing species in solution resulting in less efficient molecular tumbling and hence greater quadrupolar broadening.[24] The potassium salts are also noticeably less soluble than the sodium salts. The increased line width produces poorly resolved spectra for the potassium salts in particular, and the main group of resonances becomes a broad single feature.

In order to establish the possibility of the chemical shifts of the carborane cages depending on the identity of the cation, it was necessary to prepare solutions of lithium, sodium and potassium salts using the same solvent; d_5-pyridine reacts with the di-lithium salts so the choice was to use 10% benzene-d_6 in THF. The benzene-d_6 provides a lock without reducing the solvent polarity sufficiently to precipitate the salts; clearly such a solvent can only be used to obtain ^{11}B and ^{13}C NMR spectra. Solutions of the sodium and potassium salts in 10% C_6D_6–THF were prepared in NMR tubes by treating an excess of NaH or KH with a solution of 7,8-$C_2B_9H_{13}$, $(HNMe_3)$(7,9-$C_2B_9H_{12}$) or 2,9-$C_2B_9H_{13}$. Solutions of the di-lithium salts were similarly prepared by the reaction of the carborane precursors in 10% C_6D_6–THF with a slight excess over two equivalents of BuLi in hexanes.

Tables 1–3 list the ^{11}B NMR data for the lithium, sodium and potassium salts **1**–**9** recorded in THF–10% C_6D_6. 2D ^{11}B–^{11}B COSY spectra on these solutions were uninformative except for the spectrum corresponding to the salt Li_2(7,9-$C_2B_9H_{11}$) **4** which enabled each peak to be assigned. The latter COSY spectrum is depicted in the ESI†. The ^{11}B{^{1}H} spectra themselves appear in Fig. 4 for the salts M_2(7,8-$C_2B_9H_{11}$) **1**–**3**, Fig. 5 for M_2(7,9-$C_2B_9H_{11}$) **4**–**6** and Fig. 6 for M_2(2,9-$C_2B_9H_{11}$) **7**–**9**. Assuming that the cage atoms do not rearrange, the ^{11}B NMR spectra for salts from 2,9-$C_2B_9H_{13}$ would have the expected 2 : 2 : 2 : 2 : 1 ratio with the unique peak assigned to the boron antipodal to the naked vertex (*i.e.*, the open face) in the *nido*-carborane. Therefore the low frequency resonances in $M_2C_2B_9H_{11}$ are assigned to the boron atom B1 with respect to the *nido*-C_2B_9-cage numbering, and their chemical shift strongly reflects the electronic changes at the open face of the C_2B_9-cage.

Table 7 Relative energies of MP2/6-31G* optimised geometries **A–FF**

Optimised geometries		ZPE/a.u (NIMAG)	MP2 energy/a.u.	Relative energy/kcal mol^{-1}
7,8-$C_2B_9H_{11}^{2-}$	**A**	102.51(0)	−305.35514	16.33
7,9-$C_2B_9H_{11}^{2-}$	**B**	102.59(0)	−305.38128	0.00
2,9-$C_2B_9H_{11}^{2-}$	**C**	102.08(0)	−305.33805	26.67
2,3-$(Me_3Si)_2$-2,3-$C_2B_4H_4^{2-}$	**D**	189.68(0)	−993.81444	30.6
2,4-$(Me_3Si)_2$-2,4-$C_2B_4H_4^{2-}$	**E**	189.25(0)	−993.85359	0.0
7,8-Me_2-7,8-$C_2B_9H_{11}^{2-}$	**F**	139.69(0)	−383.69665	
ap-Na-7,8-Me_2-7,8-$C_2B_9H_9^-$	**G**	141.79(0)	−545.69498	
4,5-*exo*-(en)Li-*ap*-(en)Li-2,3-$(H_3Si)_2$-2,3-$C_2B_4H_4$	**H**	233.32(0)	−1153.71669	22.2
5,6-*exo*-(en)Li-*ap*-(en)Li-2,4-$(H_3Si)_2$-2,4-$C_2B_4H_4$	**I**	233.53(0)	−1153.74681	0.0
4,5-*exo*-Li-*ap*-Li-2,3-$(H_3Si)_2$-2,3-$C_2B_4H_4$	**J**	80.14(0)	−773.86862	20.5
5,6-*exo*-Li-*ap*-Li-2,4-$(H_3Si)_2$-2,4-$C_2B_4H_4$	**K**	80.33(0)	−773.89628	0.0
4,5-*exo*-Li-2,3-$(H_3Si)_2$-2,3-$C_2B_4H_4^-$	**P**	76.97(0)	−766.36401	26.0
5,6-*exo*-Li-2,4-$(H_3Si)_2$-2,4-$C_2B_4H_4^-$	**Q**	77.37(0)	−766.39904	0.0
ap-Li-2,3-$(Me_3Si)_2$-2,3-$C_2B_4H_4^-$	**L**	193.89(0)	−1001.47604	29.3
ap-Li-2,4-$(Me_3Si)_2$-2,4-$C_2B_4H_4^-$	**M**	193.44(0)	−1001.51272	0.0
1,4,5-*exo*-Na-*ap*-Na-2,3-$(H_3Si)_2$-2,3-$C_2B_4H_4$	**R**	77.94(0)	−1082.63655	21.8
1,5,6-*exo*-Na-*ap*-Na-2,4-$(H_3Si)_2$-2,4-$C_2B_4H_4$	**S**	78.09(0)	−1082.66618	0.0
ap-Na-2,3-$(Me_3Si)_2$-2,3-$C_2B_4H_4^-$	**N**	192.49(0)	−1155.84452	28.7
ap-Na-2,4-$(Me_3Si)_2$-2,4-$C_2B_4H_4^-$	**O**	192.00(0)	−1155.87913	0.0
1,4,5-*exo*-Na-2,3-$(Me_3Si)_2$-2,3-$C_2B_4H_4^-$	**T**	191.48(0)	−1155.81200	46.4
1,5,6-*exo*-Na-2,4-$(Me_3Si)_2$-2,4-$C_2B_4H_4^-$	**U**	190.93(0)	−1155.85267	16.4
1,4,5-*exo*-(en)Na-*ap*-(en)Na-2-(H_3Si)-3-Me-2,3-$C_2B_4H_4$	**V**	239.25(0)	−1211.45913	0.6
1,5,6-*exo*-(en)Na-*ap*-(en)Na-2-(H_3Si)-3-Me-2,3-$C_2B_4H_4$	**W**	239.25(0)	−1211.46020	0.0
ap-Li-7,8-$C_2B_9H_{11}^-$	**X**	106.49(0)	−312.98927	16.75
ap-Li-7,9-$C_2B_9H_{11}^-$	**Y**	106.70(0)	−313.01626	0.00
ap-Li-2,9-$C_2B_9H_{11}^-$	**Z**	106.62(0)	−312.99122	15.64
ap-Na-7,8-$C_2B_9H_{11}^-$	**AA**	104.75(0)	−467.35702	15.52
ap-Na-7,9-$C_2B_9H_{11}^-$	**BB**	104.96(0)	−467.38206	0.00
ap-Na-2,9-$C_2B_9H_{11}^-$	**CC**	104.76(0)	−467.35379	17.55
5,6,10-*exo*-Li-*ap*-Li-7,8-$C_2B_9H_{11}$	**DD**	108.64(0)	−320.45291	9.61
6,10,11-*exo*-Li-*ap*-Li-7,9-$C_2B_9H_{11}$	**EE**	108.61(0)	−320.46819	0.00
3,7,8-*exo*-Li-*ap*-2,9-Li$C_2B_9H_{11}$	**FF**	108.48(0)	−320.43604	20.05

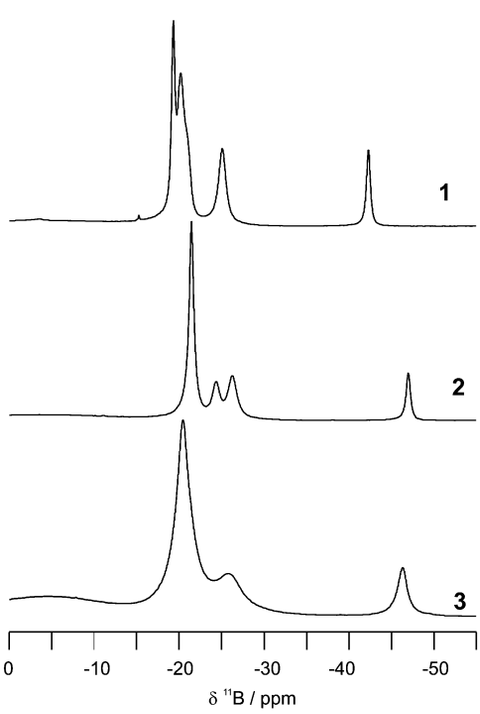

Fig. 4 The 96.2 MHz $^{11}B\{^1H\}$ NMR spectra of $M_2(7,8\text{-}C_2B_9H_{11})$ (M = Li, Na, K) **1**–**3** recorded in THF–10% C_6D_6.

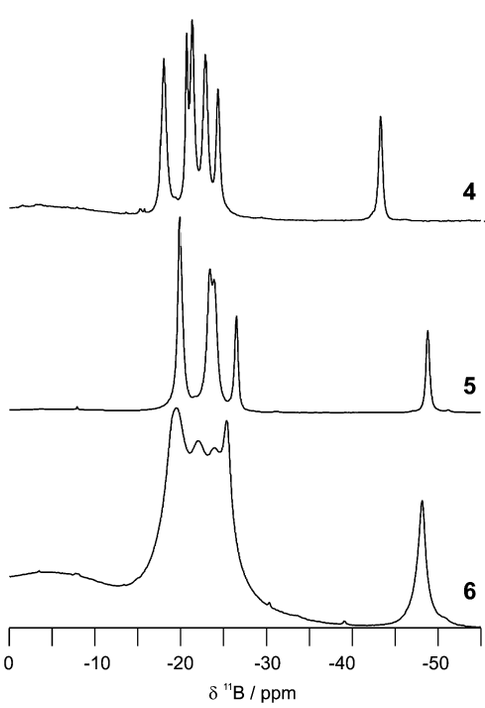

Fig. 5 The $^{11}B\{^1H\}$ NMR spectra of $M_2(7,9\text{-}C_2B_9H_{11})$ (M = Li, Na, K) **4**–**6** recorded in THF–10% C_6D_6.

For each salt it is clear that the low frequency ^{11}B resonance undergoes a significant change in chemical shift as the cation is varied. The previously reported ^{11}B NMR data for $Li_2(7,8\text{-}C_2B_9H_{11})$ **1** in d_8-THF are in agreement with our findings but for $Na_2(7,8\text{-}C_2B_9H_{11})$ **2** the 6 : 1 : 1 : 1 ratio of the resonances reported[8] is in fact 5 : 1 : 2 : 1 after careful inspection of the peak intensities.

For the di-lithium and di-sodium salts of the smaller cage dianions, **10**, **11**, **12**, **13** and the unsolvated di-lithium salt $Li_2[2,3\text{-}(Me_3Si)_2\text{-}2,3\text{-}C_2B_4H_4]$ **14**, there are trends in the observed chemical shifts of the apical boron atoms (*i.e.*, B1) on varying the cation and on varying the solvent (Table 4 and Table 5). It is interesting to note that the reported shifts for salts containing the monoanions $[2,3\text{-}(Me_3Si)_2\text{-}2,3\text{-}C_2B_4H_5]^-$ and $[2,4\text{-}(Me_3Si)_2\text{-}2,4\text{-}C_2B_4H_5]^-$ are only 5 ppm to high field compared to the salts (**10**, **13** and **14**) of the dianions. By contrast, in the 11-vertex carboranes shown here, there are significant differences between the ^{11}B NMR chemical shifts of the alkali

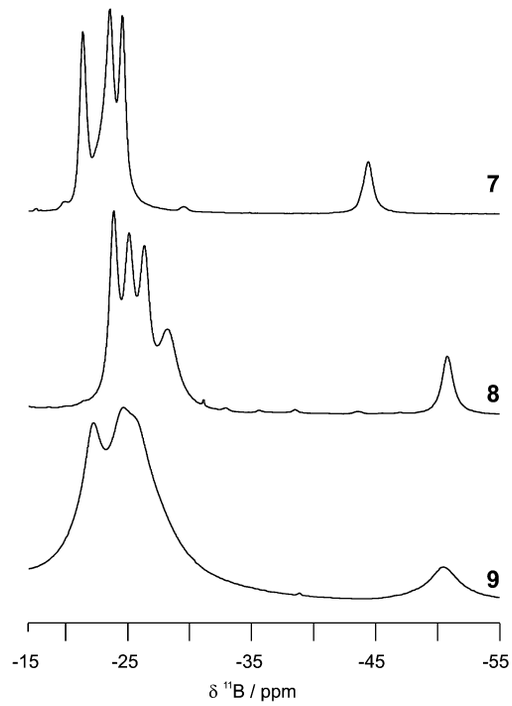

Fig. 6 The 96.2 MHz $^{11}B\{^1H\}$ NMR spectra of $M_2(2,9\text{-}C_2B_9H_{11})$ (M = Li, Na, K) **7**–**9** recorded in THF–10% C_6D_6.

metal salts of the monoanions $C_2B_9H_{12}^-$ and the corresponding dianions $C_2B_9H_{11}^{2-}$.

The ^{7}Li NMR spectra of the $Li_2C_2B_9H_{11}$ salts **1**, **4** and **7** in CD_3CN reveal two distinct broad peaks, one much broader than the other, indicating two different environments for the lithium ions in these salts. These observations provide us with evidence that the dianion is not a discrete moiety, rather that there is some degree of covalence or strong ion-pairing between the lithium cations and the carborane anion $C_2B_9H_{11}^{2-}$. For the reported di-lithium salts **10** and **11** two broad ^{7}Li resonances were observed, with the very broad one corresponding to the *exo* lithium and the other to the apical lithium.[9,10] In the case of the lithium NMR spectra recorded for the three di-lithium salts in THF–10% C_6D_6, the salt $Li_2(7,8\text{-}C_2B_9H_{11})$ **1** reveals two broad peaks whereas the other two salts, **4** and **7**, give a single broad peak.

As spectroscopic data have been reported for so few 11-vertex carborane dianions, our attention was drawn to a report of the di-sodium salt, $Na_2(7,8\text{-}Me_2\text{-}7,8\text{-}C_2B_9H_9)$ **15**, for which the approximate ^{11}B NMR chemical shifts extracted from the published stick diagram are −27 (3B), −37 (4B), −53 (1B) and −55 (1B) ppm.[25] If the observed shifts are upfield by 20 ppm then the values are identical, within experimental error, to our NMR data (see ESI†) for the salt $(HNMe_3)(7,8\text{-}Me_2\text{-}7,8\text{-}C_2B_9H_{10})$. Given this observation, we have re-prepared $Na_2Me_2C_2B_9H_9$ **15** by the reaction of $(HNMe_3)(7,8\text{-}Me_2\text{-}7,8\text{-}C_2B_9H_{10})$ and NaH in THF–10% C_6D_6 and obtained ^{11}B NMR chemical shifts as listed in Table 6. Clearly the previously reported NMR data for **15** correspond to the monoanion, $7,8\text{-}Me_2\text{-}7,8\text{-}C_2B_9H_{10}^-$.

^{11}B NMR data for the alkali metal salts of the monoanions 7,8-, 7,9- and $2,9\text{-}C_2B_9H_{12}^-$ were carefully observed during this study and compared with virtually identical reported values.[2,15,26] They are shown to be independent of the identity of the counter-cation and solvent, indicating that the monoanions, *nido*-$C_2B_9H_{12}^-$, exist as discrete ions in solution. Similar conclusions can be reached from ^{11}B NMR data of alkali metal salts containing the monoanions $2,3\text{-}(Me_3Si)_2\text{-}2,3\text{-}C_2B_4H_5^-$ and $2,4\text{-}(Me_3Si)_2\text{-}2,4\text{-}C_2B_4H_5^-$.[12,27,28]

Theoretical studies

Fully optimised geometries at the electron correlated and computationally intensive MP2/6-31G* level of theory can be regarded as excellent representations of molecular structures found experimentally in the gas phase and in solution for carboranes.[29,30] Prior to describing the results of geometry optimisation for the dianions $C_2B_9H_{11}^{2-}$, we compare theoretical and experimental structural data of the well characterised alkali metal salts of the related smaller carborane dianions, $(Me_3Si)_2C_2B_4H_4^{2-}$ **D** and **E**, to demonstrate the validity of data on alkali metal carboranes generated from *ab initio* computations. Reported geometry optimisations of carboranes involving lithium atoms have so far been limited to $LiC_2B_4H_6^-$ and $Li_2C_2B_4H_6$ compounds (at the B3LYP/6-31G* level).[12]

The optimised model geometries (**H** and **I**, Fig. 7) of [Li-

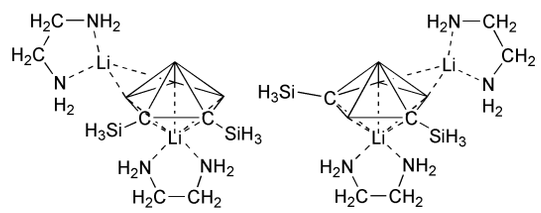

H **I**

Fig. 7 Optimised geometries of *exo*-(en)Li-*ap*-(en)Li-2,3-$(H_3Si)_2$-2,3-$C_2B_4H_4$ **H** and 5,6-*exo*-(en)Li-*ap*-(en)Li-2,4-$(H_3Si)_2$-2,4-$C_2B_4H_4$ **I** as models of **10** and **11**, respectively.

$(TMEDA)]_2[2,3\text{-}(Me_3Si)_2\text{-}2,3\text{-}C_2B_4H_4]$ **10** and $[Li(TMEDA)]_2$-$[2,4\text{-}(Me_3Si)_2\text{-}2,4\text{-}C_2B_4H_4]$ **11** were determined at the MP2/6-31G* level of theory, with each methyl group replaced by hydrogen so that TMEDA becomes ethylenediamine (en), and the structures compared with the experimental solid-state geometries. In each case the fit between experimental and theoretical geometries is very good, with misfit values of 0.0288 and 0.0247 Å for the LiC_2B_4 cage skeletons in **10** and **11**, respectively, taking into consideration the molecular simplifications employed. A comparison of bond lengths for these experimental and theoretical geometries appears in the ESI †. At the less computationally intensive level of theory B3LYP/6-31G*, the misfit values are not as good (0.0394 and 0.0256 Å for **10** and **11**, respectively).

While the experimental molecular structures of TMEDA-solvated complexes **10** and **11** show them to be discrete molecules, the structures of the THF-solvated lithium and sodium salts **12** and **13** of the $[2,4\text{-}(Me_3Si)_2\text{-}2,4\text{-}C_2B_4H_4]^{2-}$ dianion **E** are more complex (Fig. 3), with the metal atoms occupying a variety of bonding modes to give dimeric molecules. Thus, simpler optimised model geometries **J**–**U** based on the $[2,3\text{-}(Me_3Si)_2$-$2,3\text{-}C_2B_4H_4]^{2-}$ **D** and $[2,4\text{-}(Me_3Si)_2\text{-}2,4\text{-}C_2B_4H_4]^{2-}$ **E** dianions were computed and inspected and appear in Fig. 8. Two distinct bonding modes exist for the *exo*-metal atoms, a bridging mode between two basal boron atoms for lithium and a capping mode involving one apical and two basal boron atoms for sodium. The capping mode is observed in the structures of the di-sodium salt **13** and the yttracarborane complex $\{(THF)_3$-$Na\}_2\{(THF)Y(2,4\text{-}(Me_3Si)_2\text{-}2,4\text{-}C_2B_4H_4)_2\}_2$ with sodium atoms capped to the B_3 triangular faces.[31]

As the di-sodium salt of the $[2,3\text{-}(Me_3Si)_2\text{-}2,3\text{-}C_2B_4H_4]^{2-}$ dianion **D** is not known, we have examined the salt with one silyl group $[Na(TMEDA)]_2[2\text{-}(Me_3Si)\text{-}3\text{-}Me\text{-}2,3\text{-}C_2B_4H_4]$ **16**.[32] Since good agreement between the experimental and optimised geometries of TMEDA solvated di-lithium salts **10** and **11** has been demonstrated here, simplified geometries (**V** and **W**, Fig. 9) of the TMEDA solvated di-sodium salt **16** were optimised at the MP2/6-31G* level of theory. The *exo*-sodium atom in both optimised geometries **V** and **W** occupies a capping mode on the triangular face rather than the bridging mode depicted in the literature.[32] Between the two geometries **V** and **W**, the energy difference is small (*ca* 0.6 kcal mol^{-1}) with **W** being lower in energy. Thus, experimental solid-state geometries of TMEDA-

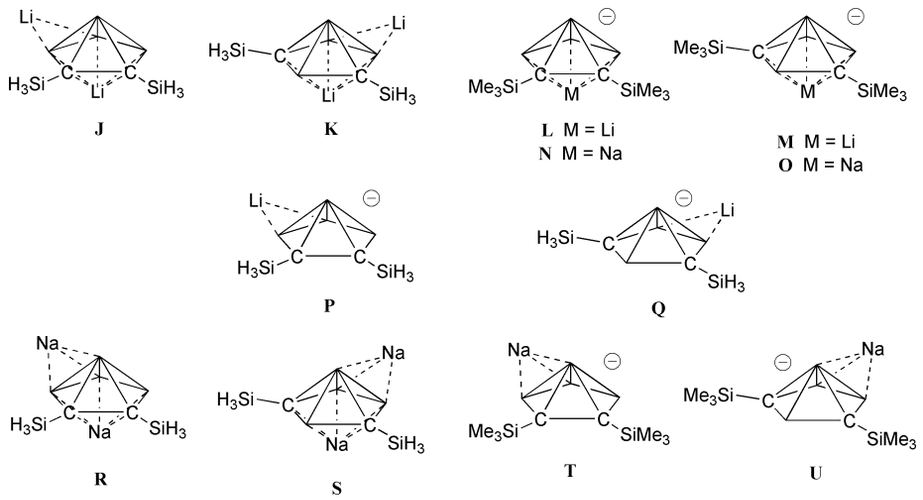

Fig. 8 Optimised model geometries **J–U**.

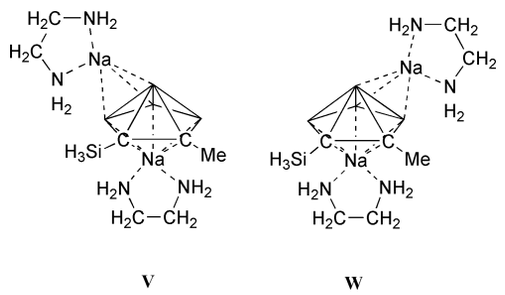

Fig. 9 Optimised geometries of 1,4,5-*exo*-(en)Na-*ap*-(en)Na-2-(H_3Si)-3-Me-2,3-$C_2B_4H_4$ **V** and 1,5,6-*exo*-(en)Na-*ap*-(en)Na-2-(H_3Si)-3-Me-2,3-$C_2B_4H_4$ **W** as models of likely geometries in the solid state for [Na(TMEDA)]$_2$[2-(Me_3Si)-3-Me-2,3-$C_2B_4H_4$] **16**.

solvated di-sodium salts such as **16** are expected to contain *exo*-capping sodium atoms.

Relative energies (Table 7) for the model geometries of the ion-pairs of smaller carboranes show the more stable geometries to be those with the metal occupying an apical position. It has to be pointed out that the effect of two or more coordinating solvent molecules such as THF and TMEDA has not been taken into account here. As expected, compounds containing the 2,4-isomer are lower in energy with respect to analogous compounds containing the 2,3-isomer.[33] The smallest difference in energy between the apical and *exo* geometries of the small carborane ion-pairs of type $MC_2B_4H_6^-$ is found in the Na-2,4-(Me_3Si)$_2$-2,4-$C_2B_4H_4^-$ geometries **O** and **U**. The stability of the two geometries could well be reversed if the sodium atom is coordinated to two or more ligand molecules. An example is demonstrated in the structurally characterised sodium salts of the monoanion, 2,4-(Me_3Si)$_2$-2,4-$C_2B_4H_5^-$, where one TMEDA molecule is attached to the apical sodium in Na(TMEDA)-2,4-(Me_3Si)$_2$-2,4-$C_2B_4H_5$ or two TMEDA molecules to the *exo* sodium in Na(TMEDA)$_2$-2,4-(Me_3Si)$_2$-2,4-$C_2B_4H_5$.[32]

Optimised geometries (at the MP2/6-31G* level of theory) of the discrete dianions $C_2B_9H_{11}^{2-}$ **A–C** were computed. Fig. 10 shows the optimised geometries of the anionic ion-pairs $MC_2B_9H_{11}^-$ (M = Li or Na) and the neutral ion-pairs $Li_2C_2B_9H_{11}$. The most stable geometries computed for the anionic ion-pairs $MC_2B_9H_{11}^-$ (M = Li or Na) are with the metal atoms at the apical positions **X–CC**. For the neutral di-lithium species $Li_2C_2B_9H_{11}$, the capping mode on the triangular boron face is favoured by the *exo*-lithium atom. The most stable neutral species are 5,6,10-*exo*-Li-*ap*-Li-7,8-$C_2B_9H_{11}$ **DD** for Li$_2$(7,8-$C_2B_9H_{11}$), 6,10,11-*exo*-Li-*ap*-Li-7,9-$C_2B_9H_{11}$ **EE** for Li$_2$(7,9-$C_2B_9H_{11}$) and 3,7,8-*exo*-Li-*ap*-Li-2,9-$C_2B_9H_{11}$ **FF** for Li$_2$(2,9-$C_2B_9H_{11}$) with the capped B_3-triangular faces between the upper and lower belts. This differs from the bridging mode observed experimentally and determined theoretically for the di-lithium

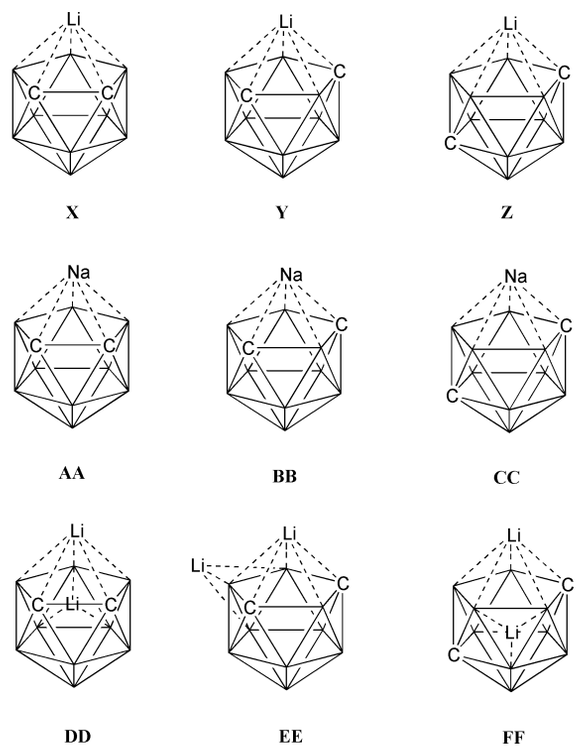

Fig. 10 Optimised geometries of the carborane ion-pairs *ap*-LiC_2-$B_9H_{11}^-$ **X–Z** and *ap*-Na$C_2B_9H_{11}^-$ **AA–CC** and the preferred geometries for the neutral carboranes $Li_2C_2B_9H_{11}$ **DD–FF**.

salts of the smaller carborane dianions **D** and **E**. Again, it has to be pointed out that the effect of coordinating solvent has not been taken into account here. As shown in Table 7, relative energies of optimised geometries for the discrete dianions $C_2B_9H_{11}^{2-}$, the anionic ion-pairs $MC_2B_9H_{11}^-$ (M = Li or Na) and the neutral ion-pairs $Li_2C_2B_9H_{11}$ show the 7,9-isomer to be the most stable form of the three isomers in all cases.

If ^{11}B NMR shifts computed at various levels (*e.g.*, IGLO, GIAO) from an optimised geometry (MP2/6-31G*) of a carborane show a very good correlation with its experimental solution-state NMR data then the optimised geometry is considered to be a good representation of its molecular structure in solution.[29] To our knowledge the accuracy of computed NMR shifts generated from optimised geometries for alkali metal salts of carborane dianions has not been demonstrated.

As ^{11}B NMR data are known for the several salts of smaller cages, calculated shifts (listed in Table 4 and Table 5) generated from the optimised geometries are compared with reported chemical shifts. In general, the tables show good correlation

between observed shifts for the di-lithium salts (**10**, **11**, **12**, **14**) and computed ^{11}B NMR chemical shifts for both the anionic ion-pairs containing lithium on the open face (**L**, **M**) and the neutral ion-pairs containing two lithium atoms (**H**, **I**, **K**, **J**). Comparison between observed and computed shifts for the 2,4-isomer derivatives in Table 5 indicates the TMEDA solvated di-lithium salt **11** to be a discrete neutral compound (geometry type **I**) in solution whereas the di-lithium salt **12** is an anionic ion-pair with one lithium atom located on the open face in THF (geometry type **M**). These results suggest computed shifts generated from optimised geometries for di-lithium salts of carborane dianions are reasonably accurate at the B3LYP/6-311G* level.

Boron chemical shifts computed for the discrete dianions (**D**, **E**), anionic ion-pairs (**N**, **O**, **T**, **U**) and neutral ion-pairs (**R**, **S**) with sodium atoms on the open face are unfortunately similar. Computed shifts of the possible geometries (**E**, **O**, **S**, **U**) for the di-sodium salt **13** in solution are deshielded by approximately 10 ppm compared to observed values. Perhaps intriguing is that **13** appears to fit best with the anionic ion-pair containing the sodium atom capped on the B_3 triangular face (geometry **U**). It is not clear whether the observed shifts for the salt **13** or the level of theory used to compute the shifts from geometries containing sodium are in error by *ca.* 10 ppm.

Theoretical ^{11}B, ^{13}C and ^{1}H NMR chemical shifts (Tables 1–3) for the optimised geometries of $C_2B_9H_{11}^{2-}$ **A–C**, $MC_2B_9H_{11}^-$ **X–CC** and $Li_2C_2B_9H_{11}$ **DD–FF** were calculated at the GIAO–B3LYP/6-311G* level. Comparison between observed and computed NMR shifts indicates that the di-lithium salts $Li_2C_2B_9H_{11}$ exist in solution as the anionic ion-pairs (M = Li). The di-sodium salts also appear to comprise the anionic ion-pairs in solution but there is little difference between the calculated shifts of the discrete dianions and the ion-pairs $NaC_2B_9H_{11}^-$ like that found for the smaller cage analogues. However the small shift changes observed for the di-sodium salts with different solvents support the presence of ion-pairs $NaC_2B_9H_{11}^-$ in solution. For the dimethyl salt, Na_2(7,8-Me_2-7,8-$C_2B_9H_9$) **15**, there is some difference in the computed shifts generated from optimised geometries of the discrete dianion 7,8-Me_2-7,8-$C_2B_9H_9^{2-}$ **F** and the ion-pair Na-7,8-Me_2-7,8-$C_2B_9H_9^-$ **G** but neither set of values fits well with observed shifts (Table 6).

Conclusions

Experimental solution-state NMR data for the nine alkali metal salts $M_2C_2B_9H_{11}$ **1**–**9** (M = Li, Na, K) in different solvents are reported here for the first time. The variation in the spectroscopic properties of the salts $M_2C_2B_9H_{11}$, as the counter-cation is changed, provides evidence that the dianion is not a discrete moiety, rather that there is some degree of covalence or strong ion-pairing between the cations and the carborane dianion $C_2B_9H_{11}^{2-}$. The experimental data for the alkali metal salts fit well with computed shifts from optimised geometries of the intimate ion-pair anions, $MC_2B_9H_{11}^-$ where the metal atom sits on the open face. Isolation of the discrete $C_2B_9H_{11}^{2-}$ dianions will require less electrophilic cations. Solid-state structures of the salts **1**–**9** are expected to contain one metal atom on the open face and one capping to a three-boron triangular face between the two belts.

For the known di-lithium and di-sodium salts of the related dianions $C_2B_4H_4(SiMe_3)_2^{2-}$, the most likely geometries in solution are the intimate ion-pair anions $MC_2B_4H_6(SiMe_3)_2^-$ with the metal atom located at the open face as suggested in an earlier study.[12] Based on geometry optimisations carried out here, the preferred bonding modes of the *exo*-metal atom in these salts are bridging at the basal boron atoms for lithium and capping at the three-boron triangular face for sodium.

Acknowledgements

We acknowledge the award of an EPSRC Advanced Research Fellowship to M. A. F. We thank EPSRC and Kvaerner Process Technology for a studentship to A. L. J.

References

1 M. F. Hawthorne, D. C. Young, T. D. Andrews, D. V. Howe, R. L. Pilling, A. D. Pitts, M. Reintjes, L. F. Warren and P. A. Wegner, *J. Am. Chem. Soc.*, 1968, **90**, 879.
2 D. C. Busby and M. F. Hawthorne, *Inorg. Chem.*, 1982, **21**, 4101.
3 N. N. Greenwood and A. Earnshaw, *Chemistry of the Elements*, Pergamon Press, Oxford, 1st edn., 1984, p. 209.
4 R. N. Grimes, *Coord. Chem. Rev.*, 2000, **200**, 773; R. N. Grimes, in *Comprehensive Organometallic Chemistry II*, ed. E. W. Abel, F. G. A. Stone and G. Wilkinson, Pergamon Press, Oxford, 1995, vol. 1, ch. 9; M. F. Hawthorne, *Acc. Chem. Res.*, 1968, **1**, 281; A. K. Saxena and N. S. Hosmane, *Chem. Rev.*, 1993, **93**, 1081.
5 J. Plešek and S. Heřmánek, *Inorg. Synth.*, 1984, **22**, 231.
6 A. K. Saxena, J. A. Maguire and N. S. Hosmane, *Chem. Rev.*, 1997, **97**, 2421.
7 R. Uhrhammer, D. J. Crowther, J. D. Olson, D. C. Swenson and R. F. Jordan, *Organometallics*, 1992, **11**, 3098.
8 M. J. Manning, C. B. Knobler, R. Khattar and M. F. Hawthorne, *Inorg. Chem.*, 1991, **30**, 2009.
9 N. S. Hosmane, A. K. Saxena, R. D. Barreto, H. Zhang, J. A. Maguire, L. Jia, Y. Wang, A. R. Oki, K. V. Grover, S. J. Whitten, K. Dawson, M. A. Tolle, U. Siriwardane, T. Demissie and J. S. Fagner, *Organometallics*, 1993, **12**, 3001.
10 H. Zhang, Y. Wang, A. K. Saxena, A. R. Oki, J. A. Maguire and N. S. Hosmane, *Organometallics*, 1993, **12**, 3933.
11 N. S. Hosmane, L. Jia, H. Zhang, J. W. Bausch, G. K. S. Prakash, R. E. Williams and T. P. Onak, *Inorg. Chem.*, 1991, **30**, 3793.
12 M. B. Ezhova, H. M. Zhang, J. A. Maguire and N. S. Hosmane, *J. Organomet. Chem.*, 1998, **550**, 409.
13 N. S. Hosmane, *J. Organomet. Chem.*, 1999, **581**, 13; G. Rana, J. A. Maguire, S. N. Hosmane and N. S. Hosmane, *Main Group Met. Chem.*, 2000, **23**, 529.
14 K. Chui, H.-W. Li and Z. Xie, *Organometallics*, 2000, **19**, 5447.
15 M. A. Fox, A. E. Goeta, J. A. K. Howard, A. K. Hughes, A. L. Johnson, D. A. Keen, K. Wade and C. C. Wilson, *Inorg. Chem.*, 2001, **40**, 173–174; M. A. Fox, A. E. Goeta, A. K. Hughes and A. L. Johnson, *J. Chem. Soc., Dalton Trans., in press.*
16 G. G. Hlatky and D. J. Crowther, *Inorg. Synth.*, 1998, **32**, 229.
17 M. F. Hawthorne, D. C. Young, P. M. Garrett, D. A. Owen, S. G. Schwerin, F. N. Tebbe and P. A. Wegner, *J. Am. Chem. Soc.*, 1968, **90**, 862.
18 J. Plešek and S. Heřmánek, *Chem. Ind. (London)*, 1973, 381.
19 D. M. Schubert, W. S. Rees Jr., C. B. Knobler and M. F. Hawthorne, *Organometallics*, 1990, **9**, 2938; J. Li, C. F. Logan and M. Jones Jr., *Inorg. Chem.*, 1991, **30**, 4866.
20 M. J. Frisch, G. W. Trucks, H. B. Schlegel, P. M. W. Gill, B. G. Johnson, M. A. Robb, J. R. Cheeseman, T. Keith, G. A. Petersson, J. A. Montgomery, K. Raghavachari, M. A. Al-Laham, V. G. Zakrzewski, J. V. Ortiz, J. B. Foresman, J. Cioslowski, B. B. Stefanov, A. Nanayakkara, M. Challacombe, C. Y. Peng, P. Y. Ayala, W. Chen, M. W. Wong, J. L. Andres, E. S. Replogle, R. Gomperts, R. L. Martin, D. J. Fox, J. S. Binkley, D. J. Defrees, J. Baker, J. P. Stewart, M. Head-Gordon, C. Gonzalez and J. A. Pople, Gaussian 94, Revision E.2, Gaussian, Inc., Pittsburgh, PA, 1995.
21 M. J. Frisch, G. W. Trucks, H. B. Schlegel, G. E. Scuseria, M. A. Robb, J. R. Cheeseman, V. G. Zakrzewski, J. A. Montgomery, Jr., R. E. Stratmann, J. C. Burant, S. Dapprich, J. M. Millam, A. D. Daniels, K. N. Kudin, M. C. Strain, O. Farkas, J. Tomasi, V. Barone, M. Cossi, R. Cammi, B. Mennucci, C. Pomelli, C. Adamo, S. Clifford, J. Ochterski, G. A. Petersson, P. Y. Ayala, Q. Cui, K. Morokuma, D. K. Malick, A. D. Rabuck, K. Raghavachari, J. B. Foresman, J. Cioslowski, J. V. Ortiz, A. G. Baboul, B. B. Stefanov, G. Liu, A. Liashenko, P. Piskorz, I. Komaromi, R. Gomperts, R. L. Martin, D. J. Fox, T. Keith, M. A. Al-Laham, C. Y. Peng, A. Nanayakkara, M. Challacombe, P. M. W. Gill, B. Johnson, W. Chen, M. W. Wong, J. L. Andres, C. Gonzalez, M. Head-Gordon, E. S. Replogle, and J. A. Pople, Gaussian 98, Revision A.9, Gaussian, Inc., Pittsburgh, PA, 1998.
22 T. P. Onak, H. L. Landesman and R. E. Williams, *J. Phys. Chem.*, 1959, **63**, 1533.
23 SHELXTL. Version 5.1., Bruker Analytical X-ray Instruments Inc., Madison, WI, 1998.

24 R. K. Harris, *Nuclear Magnetic Resonance Spectroscopy*, Longman, Harlow, 1983, p. 134.
25 P. Jutzi and P. Galow, *J. Organomet. Chem.*, 1987, **319**, 139.
26 X. L. R. Fontaine, N. N. Greenwood, J. D. Kennedy, K. Nestor, M. Thornton-Pett, S. Heřmánek, T. Jelínek and B. Štíbr, *J. Chem. Soc., Dalton Trans.*, 1990, 681; J. Plešek, B. Štíbr, X. L. R. Fontaine, J. D. Kennedy, S. Heřmánek and T. Jelínek, *Collect. Czech. Chem. Commun.*, 1991, **56**, 1618.
27 Y. Wang, H. Zhang, J. A. Maguire and N. S. Hosmane, *Organometallics*, 1993, **12**, 3781.
28 N. S. Hosmane, U. Siriwardane, G. Zhang, H. Zhu and J. A. Maguire, *J. Chem. Soc., Chem. Commun.*, 1989, 1128.
29 M. Bühl and P. v. R. Schleyer, *J. Am. Chem. Soc.*, 1992, **114**, 477; M. Bühl, J. Gauss, M. Hofmann and P. v. R. Schleyer, *J. Am. Chem. Soc.*, 1993, **115**, 12385.
30 Geometry optimisations with the MP2//6-31G* level (or similar) and computed IGLO or GIAO shifts on these geometries have been used to determine the structures of many carboranes: P. v. R. Schleyer, J. Gauss, M. Bühl, R. Greatrex and M. A. Fox, *J. Chem. Soc., Chem. Commun.*, 1993, 1766; M. A. Fox, R. Greatrex, M. Hofmann and P. v. R. Schleyer, *Angew. Chem., Int. Ed. Engl.*, 1994, **33**, 2298; D. Hnyk, D. W. H. Rankin, H. E. Robertson, M. Hofmann, P. v. R. Schleyer and M. Bühl, *Inorg. Chem.*, 1994, **33**, 4781; M. Hofmann, M. A. Fox, R. Greatrex, P. v. R. Schleyer, J. W. Bausch and R. E. Williams, *Inorg. Chem.*, 1996, **35**, 6170; M. A. Fox, R. Greatrex, M. Hofmann, P. v. R. Schleyer and R. E. Williams, *Angew. Chem., Int. Ed. Engl.*, 1997, **36**, 1498; M. A. Fox, R. Greatrex, A. Nikrahi, P. T. Brain, M. J. Picton, D. W. H. Rankin, H. E. Robertson, M. Bühl, L. Li and R. A. Beaudet, *Inorg. Chem.*, 1998, **37**, 2166; M. Hofmann, M. A. Fox, R. Greatrex, R. E. Williams and P. v. R. Schleyer, *J. Organomet. Chem.*, 1998, **550**, 331; M. A. Fox, R. Greatrex, M. Hofmann and P. v. R. Schleyer, *J. Organomet. Chem.*, 2000, **614–615**, 262; B. Wrackmeyer, H. J. Schanz, M. Hofmann and P. v. R. Schleyer, *Angew. Chem., Int. Ed. Engl.*, 1998, **37**, 1245; B. Wrackmeyer, H. J. Schanz, M. Hofmann and P. v. R. Schleyer, *Eur. J. Inorg. Chem.*, 1998, **5**, 633; B. Gangnus, H. Stock, W. Siebert, M. Hofmann and P. v. R. Schleyer, *, Angew. Chem., Int. Ed. Engl.*, 1994, **33**, 2296; J. W. Bausch, D. J. Matoka, P. J. Carroll and L. G. Sneddon, *J. Am. Chem. Soc.*, 1996, **118**, 11423; J. W. Bausch, R. C. Rizzo, L. G. Sneddon, A. E. Wille and R. E. Williams, *Inorg. Chem.*, 1996, **35**, 131; A. J. Tebben, G. Ji, R. E. Williams and J. W. Bausch, *Inorg. Chem.*, 1998, **37**, 2189.
31 N. S. Hosmane, D. Zhu, H. Zhang, A. R. Oki and J. A. Maguire, *Organometallics*, 1998, **17**, 3196.
32 N. S. Hosmane, L. Jia, Y. Wang, A. K. Saxena, H. Zhang and J. A. Maguire, *Organometallics*, 1994, **13**, 4113.
33 M. Hofmann, M. A. Fox, R. Greatrex, P. v. R. Schleyer and R. E. Williams, *Inorg. Chem.*, 2001, **40**, 1790.